

Article

Nitrogen and Organics Removal during Riverbank Filtration along a Reclaimed Water Restored River in Beijing, China

Weiyan Pan ^{1,2}, Quanzhong Huang ^{1,3,*}  and Guanhua Huang ^{1,3}

¹ Chinese-Israeli International Center for Research and Training in Agriculture China Agricultural University, Beijing 100083, China; weiyapan@126.com (W.P.); ghuang@cau.edu.cn (G.H.)

² School of Water conservancy and Environment, University of Jinan, Jinan 250022, China

³ Center for Agricultural Water Research, China Agricultural University, Beijing 100083, China

* Correspondence: huangqzh@cau.edu.cn; Tel.: +86-10-6-273-7148

Received: 30 November 2017; Accepted: 5 April 2018; Published: 17 April 2018



Abstract: Reclaimed water has been widely used to restore rivers and lakes in water scarce areas as well as in Beijing municipality, China. However, refilling the rivers with reclaimed water may result in groundwater pollution. A three-year field monitoring program was conducted to assess the effect of a riverbank filtration (RBF) system on the removal of nitrogen and organics from the Qingyang River of Beijing, which is replenished with reclaimed water. Water samples from the river, sediment, and groundwater were collected for NO₃-N, NH₄-N, and chemical oxygen demand (COD) was measured. The results indicate that about 85% of NO₃-N was removed from the riverbed sediments. Approximate 92% of NH₄-N was removed during the infiltration of water from river to aquifer. On average, 54% of COD was removed by RBF. The attenuation of NO₃-N through RBF to the groundwater varied among seasons and was strongly related to water temperature. On the other hand, no obvious temporal variability was identified in the removal of COD. These results suggest that the RBF system is an effective barrier against NO₃-N, NH₄-N and COD in the Qingyang River, as well as those rivers with similar geological and climatic conditions refilled with reclaimed water.

Keywords: chemical oxygen demand; groundwater; nitrogen; riverbank filtration

1. Introduction

Beijing faces severe problems including water scarcity and water pollution, which together are becoming key factors restricting development [1]. With the increase in scale of wastewater collection, treatment and disposal, treated wastewater has been widely reused in agricultural irrigation, landscape water and domestic supplies [2,3]. The majority of rivers have desiccated due to prolonged drought and excessive consumption. Thus, reclaimed water (i.e., treated municipal wastewater) has become a vital and inevitable water source for the urban landscape and rivers in Beijing. According to the Beijing Water Authority, more than 8×10^8 m³ of reclaimed water was utilized in 2014, accounting for 23% of total water consumption. Nearly 5×10^8 m³ of reclaimed water was used to replenish rivers and lakes [4]. According to the Surface Water Quality Standard, reclaimed water in Beijing typically meets the standard of level V2 for surface water quality, which is characterized by higher concentrations of nitrate, ammonium, salt and organic matter than those in freshwater [5,6]. Consequently, the replenishment of rivers and lakes with reclaimed water may result in groundwater contamination, which may pose a potential risk to human health. The presence and fate of organic carbon and nitrogen during bank filtration have received increased attention. Moreover, the occurrence of nitrogen and organic pollution in groundwater has been found to be a problem in Beijing and

surrounding areas in recent years. However, the environmental effects of long-term exposure to nitrate and organic compounds, especially organic micropollutants, are largely ignored. Specifically, uncertainty remains in our knowledge of the magnitude and spatial–temporal changes of nitrogen and chemical oxygen demand (COD) in groundwater in our study area.

Riverbank filtration (RBF) is a natural aquifer recharge process. It has been widely used to recover filtrated water from RBF for domestic use in recent years. As surface water flows from the river through the stream-bed and aquifer to the pumping wells, a wide variety of contaminants are naturally attenuated [7–12]. Nevertheless, the differences in hydrogeological conditions, climatic conditions and river water quality in any specific area may cause different results even with the same riverbank filtration system. Both the hydrogeological conditions and saturated/unsaturated conditions comprising the infiltration zone are important in the removal of river-borne pollutants [13]. Various biogeochemical activities take place within riverbed sediments [14]. Previous studies have found that redox conditions in sediment play an important role in altering the chemistry of infiltrating water [15]. Others have found a positive effect of available organic carbon on the denitrification rates in river sediments [16–18].

The processes of RBF that improve water quality are influenced by several factors such as temperature, redox conditions, the characteristics of the saturated zone, river water quality [19–21] and different hydrogeological conditions [22,23]. For example, seasonal changes in river flow and temperature can result in rapid changes between aerobic and anoxic conditions. The variable microbial activities under different redox conditions can affect the attenuation efficiency of water quality parameters during RBF [24]. Higher temperatures generally increase the mineralization potential [25,26]. Some researchers [19,27] have found that long flow paths and travel times between river water and pumping wells have a beneficial effect on the elimination of nitrate and organic compounds, but the presence of anoxic groundwater conditions can have undesirable effects, such as the dissolution of manganese and iron oxides and ammonification.

Reclaimed water has increasingly been used in rivers and lakes in Beijing in recent years, while the environmental risks to groundwater still remain poorly known [28,29]. The mechanism for contaminant removal and the corresponding impact factors through the RBF system with reclaimed water need to be further investigated. Therefore, a RBF system was selected, and the removal processes of $\text{NO}_3\text{-N}$, $\text{NH}_4\text{-N}$, and COD through riverbank filtration over a three-year period (2013–2015) were analyzed. The aims of the present work are to: (i) investigate the attenuation behavior of $\text{NO}_3\text{-N}$, $\text{NH}_4\text{-N}$, and COD along the infiltration path from the river to groundwater; and (ii) examine the influence of seasonal variations of environmental factors on the removal of $\text{NO}_3\text{-N}$, $\text{NH}_4\text{-N}$, and COD.

2. Materials and Methods

2.1. Site Description

The Qingyang River, which forms the principal source for the dragon-shaped water system in the Beijing Olympic Forest Park, is located at $40^\circ 00' - 40^\circ 02' \text{ N}$ and $116^\circ 22' - 116^\circ 24' \text{ E}$ at the northern end of the Beijing city axis. Qingyang River is an artificial river without natural flow, and it is refilled with reclaimed water. With a total area of 0.25 km^2 , the 9 km-long Qingyang River comprises the Qinghe diversion canal and the Yangshan drainage ditch, with the latter discharging excess water into the Qinghe River (Figure 1). The Qingyang River has been recharged by reclaimed water since 2008, with approximately $1.5 \times 10^6 \text{ m}^3$ of reclaimed water discharged into the surface system between March and November each year. The daily discharge was around $6048 \text{ m}^3/\text{d}$ during the period of reclaimed water recharge (from 15 March to 17 November in 2014). The reclaimed water was replenished into the Qingyang River via the conveyance pipeline in the northwest part of the Qinghe diversion canal, and the recharge point was 1.1 km from the sampling section (Figure 1). The recharge rate of reclaimed water was around $0.07 \text{ m}^3 \text{ s}^{-1}$.

The results of precipitation, river stage and groundwater levels are shown in Figure 2. As shown in Figure 2, the annual rainfall was 457 mm and the largest precipitation event (106 mm) was recorded on 2 September in 2014. In the early recharge period, a sudden surge in the river stage prompted an emergency release of the excess storm water from the drainage system to Qinghe River. The river stage showed subtle variation over the course of the year, with an obvious decrease occurring between August and September owing to flood discharge. The average width of the watercourse is 18.0 ± 5.0 m. As shown in Figure 2, the groundwater table is about 4.0–5.0 m below the ground surface, and was primarily influenced by river flow during the study period. At the study site, continuous infiltration of the Qingyang River through a saturated zone can be confirmed. The elevation of the river surface (around 36.4 m) is higher than the groundwater level (33.0 m), and the river channel was continuously recharged with reclaimed water for a long period, therefore, the river recharges the groundwater along the flow direction, as shown in Figure 3.

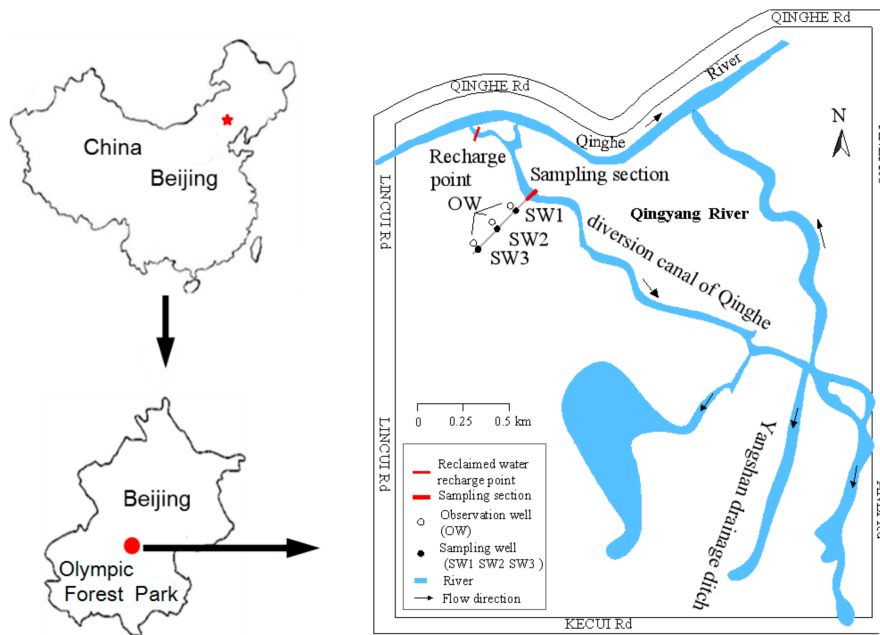


Figure 1. Location of the study site and location of sampling points.

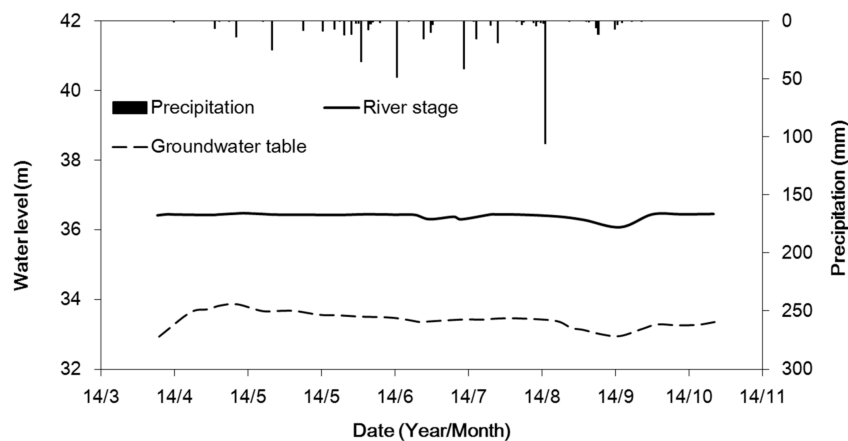


Figure 2. Variation of the river stage and groundwater table in sampling well 3 and precipitation from March to November in 2014.

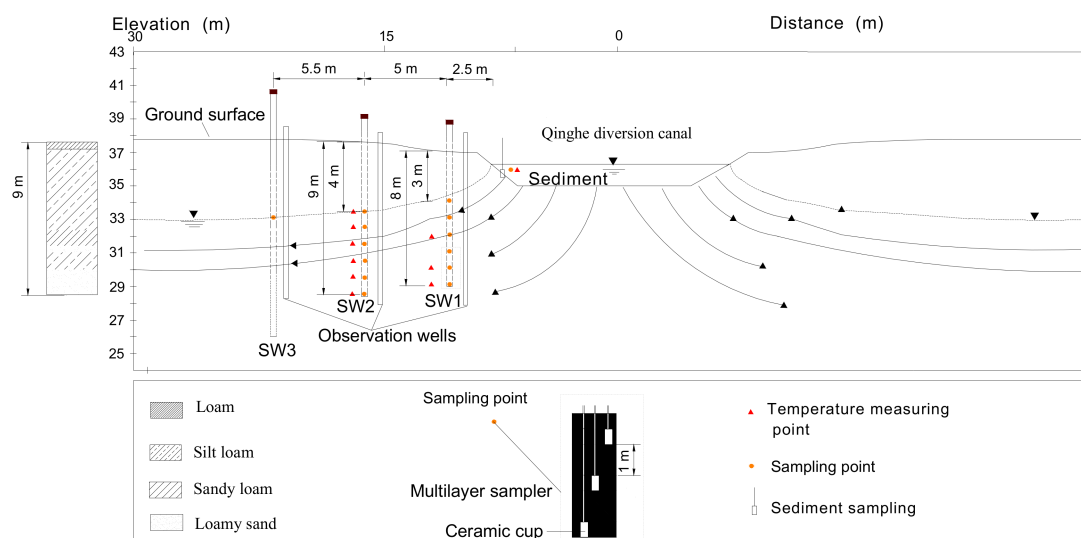


Figure 3. Schematic of the sampling points at the sampling section.

Olympic Forest Park is characterized by a natural landscape with vegetation of weeds such as *Chenopodium album*, *Eleusine indica* and *Artemisia annua*, well-maintained grass of clipped *Zoysia japonica* and artificial forestland such as *Platycladus orientalis* and *Picea asperata*. Soil samples were collected at this monitoring site at 0.2 m intervals, from the surface to a depth of 9 m. Soil particle size distribution was analyzed using a Mastersize 2000 (Malvern Instruments, Malvern, UK) and organic matter content was measured using the potassium dichromate method. Particle size distribution and organic matter content are provided in Table 1. The hydraulic conductivity (K -value, m/day) of the soil at the monitoring site was estimated by the Rosetta model developed by the United States Salinity Laboratory [30]. The soil profile exhibited a sandwich-like texture distribution. Layered heterogeneity exists in the unsaturated and saturated zones of the study area. This may cause preferential flow, however, it is difficult for us to exactly identify the pathway of preferential flow. Additionally, the biogeochemical processes in different layers of the aquifer may be different due to the difference in clay content.

Table 1. Particle size distribution and organic matter content in the soil profile at the monitoring site.

Soil Depth (cm)	Sampling Numbers (n)	Particle Size Distribution (%)			Organic Matter Content (%)	Soil Texture	K -Value (m/day)
		0.01–2 μm	2–50 μm	50–2000 μm			
0–40	6	9	47	44	3.26	Loam	0.31
40–100	9	12	52	36	2.51	Silt loam	0.31
100–160	9	12	56	32	1.24	Silt loam	0.32
160–240	12	16	65	19	1.37	Silt loam	0.20
240–320	12	12	53	35	0.42	Silt loam	0.31
320–360	6	10	59	31	0.58	Silt loam	0.40
360–520	24	15	68	17	2.88	Silt loam	0.21
520–610	15	5	27	68	0.55	Sandy loam	0.61
610–650	12	4	22	74	0.53	Loamy sand	0.75
650–750	15	10	50	40	1.78	Silt loam	0.33
750–900	24	5	18	77	0.2	Loamy sand	0.80

2.2. Water Sample Collection

Samples of reclaimed water, river water, interstitial water and groundwater were collected during the study period. Reclaimed water samples were directly collected from the conveyance pipeline, and were collected once a month from March to December in 2014. One sampling section was selected to investigate the water quality of the Qingyang River (Figure 1). River water samples were collected about 50 cm below the water surface in the sampling section. Additionally, sediment samples were collected for interstitial water using a sampling tube (made of cylindrical polyethylene, with a length

of 100 cm, and the diameter of 4 cm). The sampling points were chosen in the top 30 cm layer of the riverbed sediment in the riverbed close to the sampling section. The interstitial water was collected in the summer months (from July to September) and the winter months (from November to December) in 2014. A total of 15 sediment samples for interstitial water were taken in the riverbed during the sampling period. The mixture of samples at different locations was used as the final sediment samples for the same sampling time. Prior to analysis, water in the sediment was isolated in a laboratory via centrifuging and filtering for $\text{NO}_3\text{-N}$ and COD. Water samples in the sediment for $\text{NH}_4\text{-N}$ analysis were obtained just by the vibration and filtering process.

Three groundwater sampling wells were prepared at the sampling section (see Figure 3). Sampling wells 1 (SW1), 2 (SW2), and 3 (SW3) were located approximately 2.5, 7.5, and 13 m from the riverbank, respectively (Figure 3). Each of the wells had a diameter of 0.2 m and screened along their full length, and was installed with multilayer samplers, which were used to collect groundwater samples. The multilayer samplers consisted of ceramic cups connected to sample bottles via Polyvinyl chloride tubing with a diameter of 5 cm. The porous ceramic cups were buried at different depths in the sampling wells. Firstly, negative pressure inside the sampling bottle was created by a vacuum pump. Then, the negative pressure inside the sampling bottle caused water flow from the soil to a sampling bottle. Clusters of ceramic cups were set at the depths of 3, 4, 5, 6, 7, and 8 m in SW1 and 4, 5, 6, 7, 8, and 9 m in SW2 (see Figure 3). The diameter of SW3 was 20 cm and water samples were collected from the groundwater surface directly via a sampling bottle. River and groundwater samples were collected two to three times a month from September to December in 2013, and from March to December in 2014 and 2015, respectively.

The temperatures of the river water, interstitial water and groundwater was measured by a thermocouple sensor. The thermocouple sensors were installed at different depths in the sampling wells (SW1 and SW2). The groundwater temperature in SW1 (at the depths of 5, 7 and 8 m) and SW2 (at the depths of 4, 5, 6, 7, 8 and 9 m) were measured on site using the thermocouple sensors and recorded every 15 min with a CR3000 data logger (Campbell Scientific Australia, Garbutt, Australia) from September to December in 2013 and from March to December in 2014.

2.3. Water Quality Analysis

Water samples were transported and kept at 4 °C during shipping and storage. Reclaimed water, river water, interstitial water and groundwater samples were analyzed for $\text{NO}_3\text{-N}$, $\text{NH}_4\text{-N}$, and chemical oxygen demand (COD), pH, electrical conductivity (EC), and dissolved oxygen (DO). All samples were filtered by membrane filter (pore size 0.2 μm , H9059, Heng Odd, Beijing, China) prior to analysis. Concentrations of $\text{NO}_3\text{-N}$ and $\text{NH}_4\text{-N}$ were measured colorimetrically using a spectrophotometer (JH756 UV/Vis spectrophotometer, Shanghai, China). COD was analyzed using the spectrophotometer method (DR/2400 spectrophotometer, Loveland, CO, USA) [31]. DO in the water was measured on site with a Sension6 dissolved oxygen meter (Dr. Lange, Berlin, Germany). The pH was measured by a pH meter (PHB-4, Rex, Shanghai, China) at field condition. EC was measured by an electrical conductivity meter (DDS-307, Rex, Shanghai, China). The on-site parameter temperature, pH, and DO were detected during sampling. The removal efficiency for each pollutant is expressed as the concentration difference between different locations, e.g., the concentration difference between surface water and interstitial water, surface water and groundwater.

2.4. Statistical Analysis

With the statistical analysis, the concentration values of the water quality parameters below the detection limit ($\text{NH}_4\text{-N}$, 0.05 mg/L, $\text{NO}_3\text{-N}$, 2 mg/L, COD, 5 mg/L) were treated as the values of the detection limit. Statistical analysis was performed using the non-parametric test with SPSS 18.0 (SPSS Inc., Chicago, IL, USA). The Kruskal–Wallis test (unpaired) was used to determine whether differences existed among parameter concentrations at different sampling locations. A significant

difference ($p < 0.05$) in the p -value indicates a change in parameter concentration at different locations, whereas no significant difference among the data sets was found for cases where $p \geq 0.05$.

3. Results and Discussion

3.1. Groundwater Flow Conditions

Figure 4 shows the changing pattern of river water and groundwater temperature from 25 September to 15 October 2014. As shown in Figure 4, the river water temperature decreased with time, corresponding to the air temperature from September to October. The groundwater temperature was much lower than the river water in this period, and the groundwater temperature decreased with the increased depth in the same sampling well. The groundwater temperature varied sinusoidally with time, which was similar to that of the river water temperature (see Figure 4), indicating groundwater recharge from the river.

The infiltration rate was estimated about $6.6 \text{ m}^3 / (\text{day} \cdot \text{m})$, using the stable seepage from river equation [32]:

$$q = k (B + Ah) \quad (1)$$

where q is the infiltration rate per unit river channel ($\text{m}^3 / (\text{day} \cdot \text{m})$); k is the permeability coefficient of the river bank (m/day), $k = 0.31 \text{ m}/\text{d}$; B is the river width (m), $B = 17 \text{ m}$; h is the river depth (m), $h = 1.7 \text{ m}$; and A is the dimensionless coefficient, $A = 2.5$, which is estimated using groundwater dynamics.

The travel time of the flow path was estimated using groundwater levels obtained from the observation wells. The travel time was around 3, 10 and 30 days from river to groundwater well SW1, SW2 and SW3, respectively.

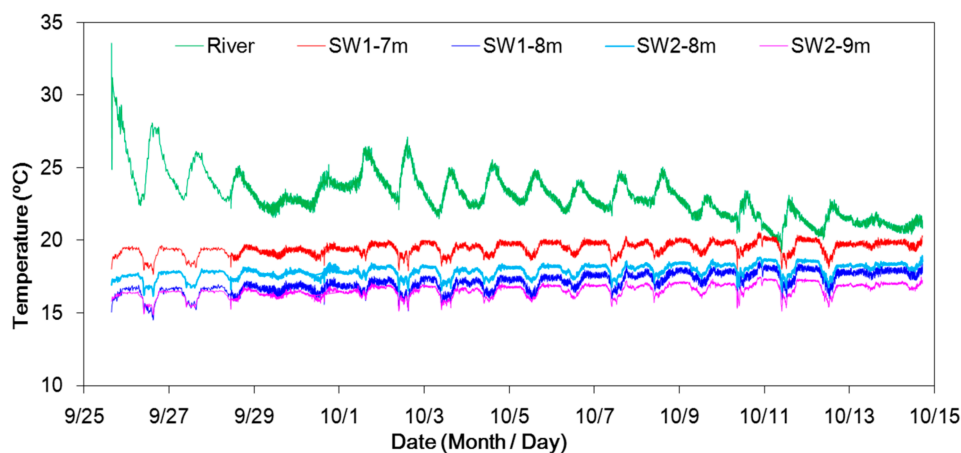


Figure 4. River water temperature and groundwater temperature from 25 September to 15 October 2014 at the depths of 7 and 8 m of sampling well 1 (SW1-7 m and SW1-8 m), and at the depths of 8 and 9 m of sampling well 2 (SW2-8 m and SW2-9 m).

3.2. Attenuation of Nitrogen and COD through the RBF System

3.2.1. Water Quality of River Water and Reclaimed Water

The concentration of $\text{NO}_3\text{-N}$, $\text{NH}_4\text{-N}$, COD, total phosphorus (TP) and total nitrogen (TN) in the reclaimed water and river water is shown in Table 2. The results indicate that the river water quality was obviously affected by reclaimed water. As shown in Figure 5, the concentration of $\text{NO}_3\text{-N}$, $\text{NH}_4\text{-N}$ and COD in the river water changed with the seasons. The $\text{NO}_3\text{-N}$ concentration in summer ($10.8 \text{ mg}/\text{L}$) was lower than that ($13.9 \text{ mg}/\text{L}$) in winter. A similar variation trend was found in the $\text{NH}_4\text{-N}$ concentration, $0.4 \text{ mg}/\text{L}$ in summer and $0.5 \text{ mg}/\text{L}$ in winter, and in the COD concentration,

15.7 mg/L in summer and 25.8 mg/L in winter. The difference in river water quality between summer and winter was attributed to the reclaimed water quality.

Table 2. Water quality of river water and reclaimed water in 2014.

Parameters	Date	NO ₃ -N (mg/L)	NH ₄ -N (mg/L)	COD (mg/L)	TP (mg/L)	TN (mg/L)	
Concentration (River water)	14 March	13.6	0.3	22.8	-	-	
	14 April	9.5	0.3	22.5	0.2	16.6	
	14 May	8.3	0.5	26.3	0.7	13.4	
	14 June	10.4	0.4	16.9	0.1	14.1	
	14 July	11.4	0.3	14.9	0.1	13.4	
	14 August	14.5	0.3	15.7	0.1	15.1	
	14 September	14.5	0.4	21.0	0.1	13.2	
	14 October	14.6	0.2	25.7	0.1	14.3	
	14 November	17.8	0.3	32.5	-	12.5	
	14 December	12.4	0.4	38.5	-	-	
	Concentration (Reclaimed water)	14 March	-	-	-	-	-
		14 April	14.8	0.2	19.6	0.5	12.2
14 May		12.5	0.4	20.6	1.0	9.0	
14 June		11.4	0.2	18.9	0.3	11.1	
14 July		12.8	0.2	11.6	0.3	10.6	
14 August		15.9	0.1	9.1	0.1	13.0	
14 September		14.9	0.3	11.6	0.1	12.5	
14 October		15.6	0.1	12.6	0.4	14.3	
14 November		18.9	0.2	18.5	-	11.8	
14 December		-	-	-	-	-	

Note: - means no data.

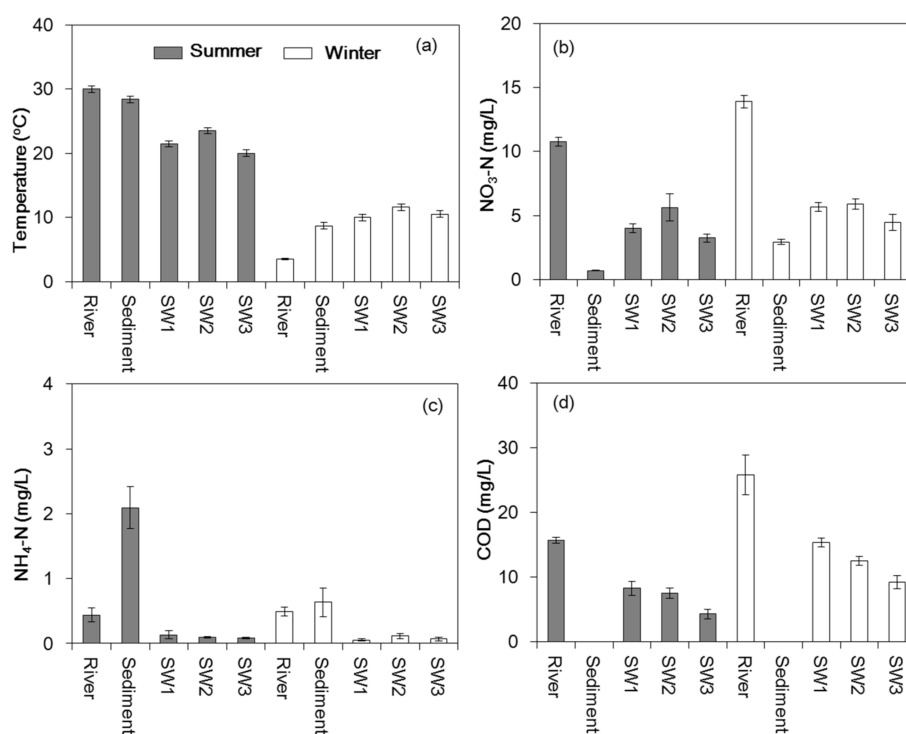


Figure 5. Mean temperature (a), NO₃-N (b), NH₄-N (c), and chemical oxygen demand (COD) (d), in river water, interstitial water and shallow groundwater in the three sampling wells (SW1, SW2, SW3) for the summer (n = 15) and winter months (n = 15) of 2014.

3.2.2. Removal of NO₃-N

The NO₃-N, NH₄-N and COD concentrations in the interstitial water and groundwater during summer and winter of 2014 are presented in Figure 5. Seasonal time periods for the site were defined as periods of uniform temperature during the summer and winter months. As shown in Figure 5b, the NO₃-N concentrations decreased significantly from 10.8 mg/L in the river water to 0.7 mg/L in the

interstitial water during the summer, and from 13.9 to 2.9 mg/L during the winter. Correspondingly, 93% and 79% of NO₃-N was removed during the infiltration of river water into sediment during summer and winter, respectively. Similarly, the DO was almost completely consumed in the sediment, dropping to <1 mg/L during infiltration. This result is consistent with that of Tufenkji et al. [33], who found that the concentrations of dissolved oxygen are highest in the overlying river water and decrease with depth in the sediment. Meanwhile, the decrease in the NO₃-N concentration of interstitial water to <2 mg/L (Figure 5b) indicates anoxic or even anaerobic conditions with considerable consumption of DO.

NO₃-N is highly soluble and easily transported from river water to the underlying sediment. In terms of a mass balance, according to Metcalf and Eddy [34], 1 g of DO is consumed as the electron acceptor for removing one gram of COD. In fact, the consumed DO along the infiltrating path was not enough for the removal of COD according to the mass balance. DO only accounted for around 37% of the total electron acceptor needed by COD removal during infiltration from the river to the groundwater. Thus, other electron acceptors were required in addition to oxygen. As previously discussed, most of the NO₃-N was consumed within the riverbed sediment. DO concentration increased from the sediment to the groundwater, indicating that NO₃-N was continuously consumed as the electron acceptor in the sediment zone. While the increase of NO₃-N during the infiltration in the zone of river bank was due to nitrification, which was proved by the reduction of NH₄-N concentration with a DO concentration higher than 2 mg/L. During this process, the NO₃-N could act as the electron acceptor and denitrification was the main process for NO₃-N removal in the sediment [35], leading to a higher NO₃-N removal efficiency. The results suggest that the sediment is an effective barrier against NO₃-N when river water recharges the groundwater.

The average temperature of the river and interstitial water in the Qingyang River was about 30 and 28 °C during the summer, and 3.5 and 8.7 °C, in the winter, respectively (Figure 5a). Although the NO₃-N concentrations in river water were considerably lower during the summer than in the winter, the NO₃-N removal efficiency through the filtration of sediment was higher in summer than in winter. This can probably be attributed to the temperature variation. Nonetheless, denitrification processes can occur anywhere in the range of 2–50 °C [36], and possibly beyond. Therefore, NO₃-N might also be removed at relatively low temperatures (5 ± 5 °C) in wintertime, because bacteria may have evolved to cope with the specific environmental conditions of our study area.

The average NO₃-N concentrations at different sampling points were significantly different, with $p = 0.001$. The average NO₃-N concentrations in the sampling wells were significantly higher than in the interstitial water ($p < 0.05$), but significantly lower than concentrations in the river water ($p < 0.05$) (Figure 5b). During the summer months, NO₃-N increased from 0.7 mg/L in interstitial water to 4.0 mg/L in the shallow groundwater from SW1 and maintained similar values at subsequent sampling wells (i.e., 5.6 mg/L in SW2 and 3.2 mg/L in SW3).

During the infiltration of river water to shallow groundwater, the NO₃-N removal efficiency was approximately 62% in SW1, 47% in SW2, and 69% in SW3. A similar pattern occurred during the winter where the removal efficiency of NO₃-N in SW1, SW2, and SW3 were 59%, 57%, and 67%, respectively. The average concentration of DO increased from 0.9 mg/L in the interstitial water to >3.0 mg/L in the surface of shallow groundwater, indicating that the reduction environment was relatively weak at the interface of the unsaturated zone and groundwater, which was also unfavorable to denitrification. In general, denitrification was promoted only when the concentration of DO fell below a certain low threshold (i.e., <1 mg/L and perhaps <2 mg/L) [37,38]. Therefore, the denitrification rates were reduced on the surface of the shallow groundwater, where DO concentrations exceeded 2 mg/L, leading to the increase of NO₃-N in the shallow groundwater compared to that of the interstitial water. Nitrification occurred as the water flowed from the sediment to the shallow aquifer, resulting in an increase in NO₃-N in the groundwater compared to that in the interstitial water. Correspondingly, as shown in Figure 5c, the NH₄-N concentration was found to decrease during infiltration from the sediment to the groundwater, indicating that NH₄-N was transformed into NO₃-N. Additionally,

the mineralization of organic nitrogen in the soil might be partly responsible for the $\text{NO}_3\text{-N}$ increase in the shallow groundwater.

3.2.3. Removal of $\text{NH}_4\text{-N}$

The average $\text{NH}_4\text{-N}$ concentrations in the interstitial water were significantly higher than those in the river water and shallow groundwater ($p < 0.05$) (Figure 5c). Specifically, the concentration of $\text{NH}_4\text{-N}$ was 0.4 mg/L (during summer) and 0.49 mg/L (during winter) in the river water, and as much as 2.1 mg/L (during summer) and 0.63 mg/L (during winter) in the interstitial water, corresponding to increases of around 425% and 28% in summer and winter, respectively. The relatively high content of clay (25%) and organic matter (1.2%) in the sediment in Qingyang River resulted in a relatively large sediment adsorption capacity. Clay containing abundant organic matter has a high cation-exchange capacity, causing a reduced $\text{NH}_4\text{-N}$ releasing flux from the sediment to the river water. In general, $\text{NH}_4\text{-N}$ can accumulate in organic-rich sediment under anaerobic conditions through ammonification by heterotrophic bacteria [39–41]. Additionally, nitrification was inhibited in a reduction condition, as the DO concentration in the interstitial water decreased to lower than 1 mg/L. The measurement might be influenced by random error due to limitations of the sampling/analytical procedure.

The average $\text{NH}_4\text{-N}$ concentrations decreased from 2 (in interstitial water) to 0.1 mg/L (in groundwater) during the summer and from 0.6 to 0.08 mg/L during the winter. As shown in Figure 5c, there was no obvious difference in $\text{NH}_4\text{-N}$ concentrations observed among the three sampling wells. Approximately 95% of the $\text{NH}_4\text{-N}$ was removed as water passed through the sediment to the shallow groundwater during the summer and 88% during the winter. The $\text{NH}_4\text{-N}$ consumption was attributed to a combination of adsorption and a subsequent nitrification process, converting $\text{NH}_4\text{-N}$ to $\text{NO}_3\text{-N}$ [42], when DO concentrations are higher than 2 mg/L. The nitrification process may partly account for the $\text{NO}_3\text{-N}$ increase in the shallow groundwater. The result was consistent with that of Essandoh et al. [37] who found that nitrification yielded high concentrations of $\text{NO}_3\text{-N}$ in the effluents during a soil column study.

3.2.4. Removal of COD

Average summertime and wintertime COD concentrations in the river water and shallow groundwater are presented in Figure 5d (note that the interstitial water samples were insufficient for COD analysis). In summer, the average COD concentration in the river water was 15.7 mg/L, decreasing to 8.3 mg/L in the shallow groundwater SW1, with a removal efficiency of 47%. In winter, the average COD concentration decreased from 25.5 to 15.3 mg/L, with a removal efficiency of 40%. The attenuation of organic compounds (as a major driver for COD) was primarily attributed to the combined effects of microbial biodegradation and adsorption onto sediments [43–45]. The COD concentrations continued to decrease in the shallow groundwater with increasing distance from the riverbank (from SW1 to SW3). The COD concentration in SW3 decreased to 4.3 mg/L in summer and 9.2 mg/L in winter. This indicates a 72.6% and 64.2% removal efficiency for summer and winter, respectively. These results are similar to those of Maeng et al. [23], who found that the removal efficiency of organic matter during bank filtration increased with residence times and travel distances. Lenk et al. [46] also demonstrated that organic matter concentrations are inversely correlated with residence times and travel distances in bank filtration sites. The COD removal efficiency was slightly higher in the summer than in the winter, which was attributed to higher temperatures, improving microbial biological activity. These results also suggest that organics can be removed at temperatures lower than 12 °C. The result is consistent with that of Abel et al. [25] who reported that the cut-off temperature to slow down or inhibit microbial activity on the attenuation of organics in soil–water systems is 5 °C.

3.3. Temporal Variations of Nitrogen and COD in Groundwater

The temporal variation of the $\text{NO}_3\text{-N}$ concentration in groundwater at depths of 5, 7, and 9 m in SW2 in 2014 is shown in Figure 6a. The variation of the $\text{NO}_3\text{-N}$ concentrations in the groundwater over time was similar to the river water concentrations. The $\text{NO}_3\text{-N}$ concentrations in the groundwater varied obviously over the sampling period. The lowest groundwater $\text{NO}_3\text{-N}$ concentrations occurred during the summer, from June to September, whereas the $\text{NO}_3\text{-N}$ concentration was relatively high during the period from March to April and from November to December. The seasonal difference in $\text{NO}_3\text{-N}$ concentration was highly dependent on denitrification, indicating that the variation of groundwater temperature was one of the important factors affecting denitrification. The groundwater temperature at different sampling depths varied from 8 to 26 °C during the experiment period (Figure 6d). High temperatures promote biological reaction (denitrification) rates and the rate of oxygen consumption [47]. Oxygen depletion through microbial activity, coupled with decreased oxygen solubility in warmer water, led to reductive conditions that were favorable to denitrification in the RBF system during the summer [20,47]. Higher temperatures and corresponding reductive conditions resulted in greater $\text{NO}_3\text{-N}$ removal during the summer than during the winter in the groundwater environment. The increase in denitrification with increasing temperature has been previously reported. Saunders and Kalff [48] reported that a 5 °C increase in temperature results in a ten-fold increase in the denitrification rate. In this study, as shown in Figure 7, the $\text{NO}_3\text{-N}$ removal efficiency increased with the groundwater temperature at an exponential function with the determination values (R^2) 0.744, 0.811, and 0.564, at depths of 5, 7, and 9 m, respectively.

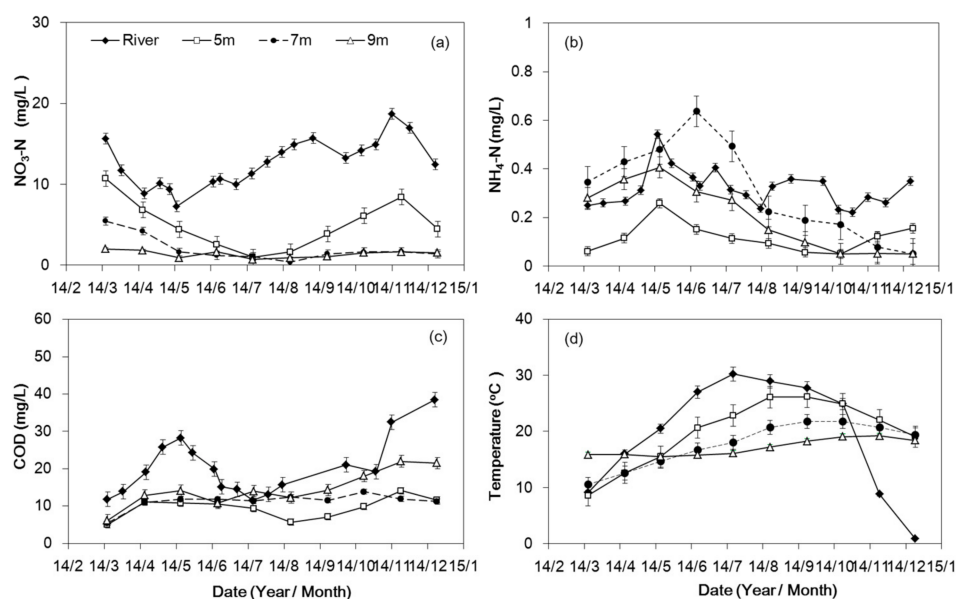


Figure 6. Temporal variations in average $\text{NO}_3\text{-N}$ (a), $\text{NH}_4\text{-N}$ (b), chemical oxygen demand (COD) (c) and temperature (d), in river water and groundwater at depths of 5, 7, and 9 m of SW2 in 2014.

Figure 6b depicts the temporal variation of $\text{NH}_4\text{-N}$ concentrations in the groundwater in 2014. The $\text{NH}_4\text{-N}$ concentrations in the groundwater varied widely over the sampling period. The $\text{NH}_4\text{-N}$ concentration increased from March to May at 5 and 9 m depth, with a temperature range from 8–16 °C (Figure 6b,d). The $\text{NH}_4\text{-N}$ concentration at 7 m depth increased from 0.35 mg/L in March to 0.64 mg/L in June, which exceeded the drinking water standard (<0.5 mg/L in China). This suggests that the $\text{NH}_4\text{-N}$ concentration in groundwater increased with groundwater temperature when the groundwater temperature was from 8–16 °C. The increase in the $\text{NH}_4\text{-N}$ concentration was mainly attributed to the mineralization of organic nitrogen. The increase in temperature enhanced the mineralization

potential [25]. Several field studies [49–51] also found that $\text{NH}_4\text{-N}$ originated from degrading in situ organic matter in the soil.

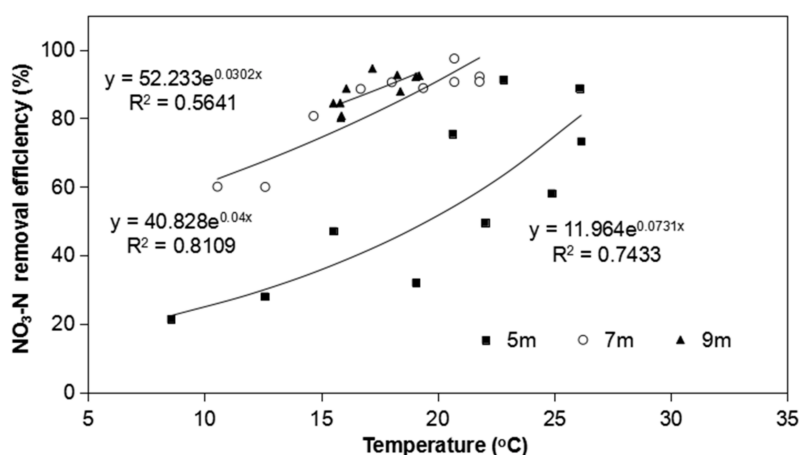


Figure 7. The relationship between $\text{NO}_3\text{-N}$ removal efficiency and groundwater temperature.

The ammonium concentration began to decline in July at three sampling depths with groundwater temperatures within a range of 20–26 °C (Figure 6b). In general, nitrification is unlikely to occur in the saturated zone with an anaerobic environment. Therefore, the decrease of $\text{NH}_4\text{-N}$ in the groundwater may be attributed to the dissociation of $\text{NH}_4\text{-N}$ to ammonia. Li et al. [52] found that $\text{NH}_4\text{-N}$ can deprotonate to ammonia in conditions with a pH value larger than 6, and the ammonia product can degas, particularly with water temperatures in a range of 19–27 °C. In this study, the pH range was from 6.7 to 8.1 in the groundwater. Under such conditions, $\text{NH}_4\text{-N}$ is likely to be degassed by a reaction of NH_4^+ (aq)– NH_3 (aq)– NH_3 (g) and emitted from the groundwater to the unsaturated pore space [53]. However, the $\text{NH}_4\text{-N}$ in the groundwater cannot be depleted completely, which is possibly explained by a release of $\text{NH}_4\text{-N}$ from organic material that balances the loss of ammonia.

The temporal variation of COD concentrations is presented in Figure 6c. The COD concentrations varied with time and showed similar variation trends at different depths. The COD concentration range was between 5.0–22.0 mg/L for three depths, which was always lower than that in the river water, which had a range of 12.8–38.5 mg/L. As shown in Figure 6c,d, the groundwater temperature varied from 8.5–26.4 °C and it did not show a significant influence on the variation of COD concentration. In contrast, Abel et al. [25] carried out a laboratory experiment and found that the dissolved oxygen carbon removal increased by 10% for every 5 °C increase in temperature over a range of 15–25 °C, whereas Hoppe-Jones et al. [24] reported that the total organic carbon concentration in the monitoring well of a RBF system was independent of season, with temperatures varying from 7–19 °C. Possemiers et al. [54] also found that temperature had hardly any effect on organic matter in groundwater when the groundwater temperature change was lower than 15 °C. In this study, the results indicate that there was no seasonal variation in COD concentration when the temperature difference was around 18 °C, that is, when the groundwater temperature varied from 8.5–26.5 °C.

3.4. Vertical Distribution of Nitrogen and COD

Figure 8 shows the average annual $\text{NO}_3\text{-N}$, $\text{NH}_4\text{-N}$ and COD concentrations in the groundwater at depths of 4–9 m during the three year period. The vertical distribution of the $\text{NO}_3\text{-N}$ concentration in 2014 was higher than in the other two experimental years due to the relatively high $\text{NO}_3\text{-N}$ concentration in river water. The $\text{NO}_3\text{-N}$ concentration decreased with depth in the saturated zone (Figure 8a). At 9 m depth, the $\text{NO}_3\text{-N}$ concentration was 1.1, 1.3, and 0.4 mg/L in 2013, 2014, and 2015, respectively. These values are much lower than the threshold for the quality standard of drinking water (10 mg/L for China). It should be noted that $\text{NO}_3\text{-N}$ removal by denitrification mainly occurred

at depths of 4–7 m for three years. Variations of $\text{NO}_3\text{-N}$ concentration at different depths are related to the corresponding soil textures. As shown in Table 1, the soil texture at the depths of 3.6–5.2 m and 6.5–7.5 m is silt loam, which causes a full denitrification process with lower saturated hydraulic conductivity and longer hydraulic retention time. The relatively high organic content (Table 1) at depths of 3.6–5.2 m and 6.5–7.5 m also resulted in an obvious $\text{NO}_3\text{-N}$ reduction in the saturated zone. This is consistent with the previous findings of Krause et al. [55] and Barnes et al. [56], who indicated that the denitrification rates and $\text{NO}_3\text{-N}$ concentrations are related to the availability of oxidizable labile organic carbon.

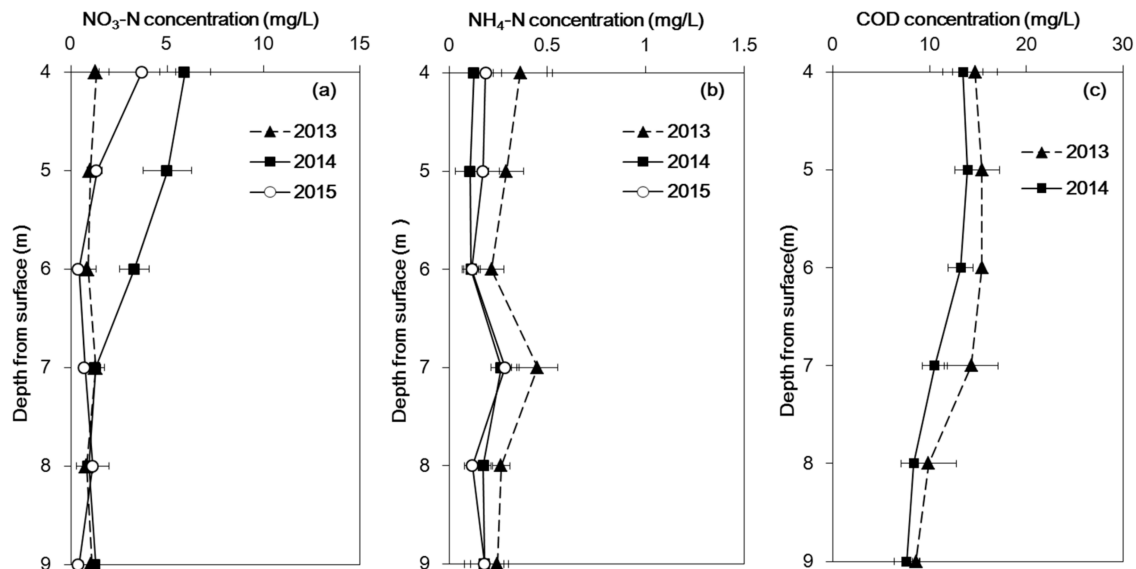


Figure 8. Vertical distributions of annual mean $\text{NO}_3\text{-N}$ (a), $\text{NH}_4\text{-N}$ (b) and chemical oxygen demand (COD) (c), in the groundwater in 2013, 2014 and 2015.

As shown in Figure 8b, the average $\text{NH}_4\text{-N}$ concentration varied with depth in the saturated zone. The $\text{NH}_4\text{-N}$ concentration profiles presented a similar change pattern for the three years. The $\text{NH}_4\text{-N}$ concentration in 2013 was higher than the other years, which was probably due to the relatively high $\text{NH}_4\text{-N}$ concentration in river water. A relatively high $\text{NH}_4\text{-N}$ concentration can be found at depths of 6–7 m. This may be attributed to the mineralization of organic nitrogen. As shown in Table 1, the relatively large amounts of organic contents found in the saturated zone at depths of 6.5–7.5 m may have led to the increase in $\text{NH}_4\text{-N}$ concentration. A similar result was found by Jiao et al. [50], who reported that the large amount of total organic carbon in the aquitard is favorable for organic nitrogen mineralization. They also found that organic nitrogen can convert to $\text{NH}_4\text{-N}$ in the aquitard. The results showed that the soil texture and organic contents varied at different depths, leading to variations of $\text{NH}_4\text{-N}$ concentration with depth in the saturated zones.

The average annual vertical distribution of the COD concentration in 2013 and 2014 is presented in Figure 8c. The COD concentration decreased with depth from 14.7 mg/L at 4 m to 8.6 mg/L at 9 m in 2013, and from 13.5 mg/L at 4 m to 7.6 mg/L at 9 m in 2014. Compared with the river water, a removal efficiency of 58.6% in 2013 and 54.6% in 2014 was found for COD at 9 m through the RBF system. Possible mechanisms for COD removal include adsorption and biodegradation during river bank filtration [25,57]. These results suggest that the RBF system is effective in COD reduction. Previous laboratory and field studies [37,57,58] have reported similar results. For example, Wang et al. [59] found that about 48–51% of the COD was removed in a laboratory column experiment. In this study, in the upper part of the shallow groundwater, the COD concentration increased slightly from 4 to 5 m. The COD concentration decreased with depth in the saturated zone (from 5 to 9 m). Different variations were attributed to the variable redox conditions under various hydrogeochemical

environments. This implies that further study is required to investigate the oxidation-reduction potential at different depths in the saturated zone in this study area.

4. Conclusions

Three-year field datasets were collected and analyzed to investigate the effect of RBF on the removal of the nitrogen and organic contaminants in the Qingyang River of Beijing. The following conclusions can be drawn:

(1) The seasonal variation exhibited an improved attenuation between winter and summer operations. A high NO₃-N removal efficiency (85%) was obtained through RBF at high temperatures (27 °C) during the summer season in Beijing.

(2) An average 54% of COD was removed through RBF. Temperature does not show a significant effect on COD removal by the RBF, whereas COD removal increases with the retention time and/or travel distance in the RBF system.

(3) The study indicates that the RBF system is an effective barrier removing NO₃-N, NH₄-N and COD in the Qingyang River. As the river was refilled with reclaimed waste water, the potential contamination risk of NO₃-N and COD for the shallow groundwater near the Qingyang River was relatively low during the monitoring period. However, long-term field observations and assessments of the RBF performance are needed to consider the safe reuse of reclaimed waste water in rivers for managed aquifer recharge. These should also include other variables such as micropollutants, the importance of travel time and general groundwater flow conditions.

Acknowledgments: This research was supported by the National Key Research and Development Project (Grant number: 2016YFC0501304) and National Natural Science Foundation of China (Grant numbers: 51639009, 51779256).

Author Contributions: Quanzhong Huang and Weiyang Pan conceived and designed the experiments; Weiyang Pan performed the experiment, analyzed the data, and wrote the paper; Guanhua Huang and Quanzhong Huang corrected and improved it.

Conflicts of Interest: The authors declare no conflicts of interest.

References

1. Chu, J.Y.; Chen, J.N.; Wang, C.; Fu, P. Wastewater reuse potential analysis: Implications for China's water resources management. *Water Res.* **2004**, *38*, 2746–2756. [[CrossRef](#)] [[PubMed](#)]
2. Yu, Y.L.; Song, X.F.; Zhang, Y.H.; Zheng, F.D.; Liu, L.C. Impact of reclaimed water in the watercourse of Huai River on groundwater from Chaobai River basin, Northern China. *Front. Earth Sci.* **2017**, *11*, 643–659. [[CrossRef](#)]
3. Ernst, M.; Sperlich, A.; Zheng, X.; Gan, Y.; Hu, J.; Zhao, X.; Wang, J.; Jekel, M. An integrated wastewater treatment and reuse concept for the Olympic Park 2008, Beijing. *Desalination* **2007**, *202*, 293–301. [[CrossRef](#)]
4. Fan, Q.; Liu, W.; Jiao, Z.; Sun, F. *Beijing Water Resources Bulletin*; Beijing Hydrological Station: Beijing, China, 2015.
5. Huang, X.R.; Xiong, W.; Liu, W.; Guo, X.Y. Effect of reclaimed water effluent on bacterial community structure in the *Typha angustifolia* L. rhizosphere soil of urbanized riverside wetland, China. *J. Environ. Sci.* **2017**, *55*, 58–68. [[CrossRef](#)] [[PubMed](#)]
6. Chen, W.P.; Lu, S.D.; Jiao, W.T.; Wang, M.E.; Chang, A.C. Reclaimed water: A safe irrigation water source? *Environ. Dev.* **2013**, *8*, 74–83. [[CrossRef](#)]
7. Ray, C.; Grischek, T.; Schubert, J.; Wang, J.Z.; Speth, T.F. A perspective of riverbank filtration. *J. Am. Water Works Assoc.* **2002**, *94*, 149–160. [[CrossRef](#)]
8. Tyagi, S.; Dobhal, R.; Kimothi, P.C.; Adlakha, L.K.; Singh, P.; Uniyal, D.P. Studies of river water quality using river bank filtration in Uttarakhand, India. *Water Qual. Expo. Health* **2013**, *5*, 139–148. [[CrossRef](#)]
9. Voeroesmary, C.J.; McIntyre, P.B.; Genssner, M.O.; Dudgeon, D.; Prusevich, A.; Green, P.; Bunn, E.S.; Sullivan, A.C.; Liermann, R.C.; Davies, M.P. Global threats to human water security and river biodiversity. *Nature* **2010**, *467*, 555–561. [[CrossRef](#)] [[PubMed](#)]
10. Ray, C. Worldwide potential of riverbank filtration. *Clean Tech. Environ. Policy* **2008**, *10*, 223–225. [[CrossRef](#)]
11. Schiermeier, Q. Water on tap. *Nature* **2014**, *510*, 326–328. [[CrossRef](#)] [[PubMed](#)]

12. Hu, B.; Teng, Y.G.; Zhai, Y.Z.; Zuo, R.; Li, J.; Chen, H.Y. Riverbank filtration in China: A review and perspective. *J. Hydrol.* **2016**, *541*, 914–927. [[CrossRef](#)]
13. Hiscock, K.M.; Grischek, T. Attenuation of groundwater pollution by bank filtration. *J. Hydrol.* **2002**, *266*, 139–144. [[CrossRef](#)]
14. Hayakawa, A.; Ikeda, S.; Tsushima, R.; Ishikawa, Y.; Hidaka, S. Spatial and temporal variations in nutrients in water and riverbed sediments at the mouths of rivers that enter Lake Hachiro, a shallow eutrophic lake in Japan. *Catena* **2015**, *133*, 486–494. [[CrossRef](#)]
15. Maeng, S.K.; Sharma, S.K.; Lekkerkerker-Teunissen, K.; Amy, G.L. Occurrence and fate of bulk organic matter and pharmaceutically active compounds in managed aquifer recharge: A review. *Water Res.* **2011**, *45*, 3015–3033. [[CrossRef](#)] [[PubMed](#)]
16. Carrey, R.; Rodriguez-Escales, P.; Otero, N.; Ayora, C.; Soler, A.; Gómez-Alday, J.J. Nitrate attenuation potential of hypersaline lake sediments in central Spain: Flow-through and batch experiments. *J. Contam. Hydrol.* **2014**, *164*, 323–337. [[CrossRef](#)] [[PubMed](#)]
17. Herrman, K.S.; Bouchard, V.; Moore, R.H. Factors affecting denitrification in agricultural headwater streams in Northeast Ohio, USA. *Hydrobiologia* **2008**, *598*, 305–314. [[CrossRef](#)]
18. Laverman, A.M.; Garnier, J.A.; Mounier, E.M.; Roose-Amsaleg, C.L. Nitrous oxide production kinetics during nitrate reduction in river sediments. *Water Res.* **2010**, *44*, 1753–1764. [[CrossRef](#)] [[PubMed](#)]
19. Grischek, T.; Hiscock, K.M.; Metschies, T.; Dennis, P.F.; Nestler, W. Factors affecting denitrification during infiltration of river water into a sand and gravel aquifer in Saxony, Germany. *Water Res.* **1998**, *32*, 450–460. [[CrossRef](#)]
20. Filter, J.; Jekel, M.; Ruhl, A.S. Impacts of accumulated particulate organic matter on oxygen consumption and organic micro-pollutant elimination in bank filtration and soil aquifer treatment. *Water* **2017**, *9*, 349. [[CrossRef](#)]
21. Schoenheinz, D.; Grischek, T. *Behavior of Dissolved Organic Carbon During Bank Filtration under Extreme Climate Conditions*; Springer: Dordrecht, The Netherlands, 2011; pp. 51–67. [[CrossRef](#)]
22. Bertelkamp, C.; Verliefde, A.R.D.; Schoutteten, K.; Vanhaecke, L.; Vanden, B.J.; Singhal, N.; van der Hoek, J.P. The effect of redox conditions and adaptation time on organic micropollutant removal during river bank filtration: A laboratory-scale column study. *Sci. Total Environ.* **2016**, *544*, 309–318. [[CrossRef](#)] [[PubMed](#)]
23. Maeng, S.K.; Ameda, E.; Sharma, S.K.; Grützmacher, G.; Amy, G.L. Organic micropollutant removal from wastewater effluent-impacted drinking water sources during bank filtration and artificial recharge. *Water Res.* **2010**, *44*, 4003–4014. [[CrossRef](#)] [[PubMed](#)]
24. Hoppe-Jones, C.; Oldham, G.; Drewes, J.E. Attenuation of total organic carbon and unregulated trace organic chemicals in U.S. riverbank filtration systems. *Water Res.* **2010**, *44*, 4643–4659. [[CrossRef](#)] [[PubMed](#)]
25. Abel, C.D.T.; Sharma, S.K.; Malolo, Y.N.; Maeng, S.K.; Kennedy, M.D.; Amy, G.L. Attenuation of bulk organic matter, nutrients (N and P), and pathogen indicators during soil passage: Effect of temperature and redox conditions in simulated soil aquifer treatment (SAT). *Water Air Soil Pollut.* **2014**, *223*, 5205–5220. [[CrossRef](#)]
26. Grünheid, S.; Amy, G.; Jekel, M. Removal of bulk dissolved organic carbon (DOC) and trace organic compounds by bank filtration and artificial recharge. *Water Res.* **2005**, *39*, 3219–3228. [[CrossRef](#)] [[PubMed](#)]
27. Im, H.; Yeo, I.; Maeng, S.K.; Park, C.H.; Choi, H. Simultaneous attenuation of pharmaceuticals, organic matter, and nutrients in wastewater effluent through managed aquifer recharge: Batch and column studies. *Chemosphere* **2016**, *143*, 135–141. [[CrossRef](#)] [[PubMed](#)]
28. Yang, L.; He, J.T.; Liu, Y.; Wang, J.; Jiang, L.; Wang, G.C. Characteristics of change in water quality along reclaimed water intake area of the Chaobai River in Beijing, China. *J. Environ. Sci.* **2015**, *50*, 93–102. [[CrossRef](#)] [[PubMed](#)]
29. Li, Z.; Xiang, X.; Li, M.; Ma, Y.P.; Wang, J.H.; Liu, X. Occurrence and risk assessment of pharmaceuticals and personal care products and endocrine disrupting chemicals in reclaimed water and receiving groundwater in China. *Ecotoxicol. Environ. Saf.* **2015**, *119*, 74–80. [[CrossRef](#)] [[PubMed](#)]
30. Schaap, M.G.; Leij, F.J.; van Genuchten, M.T. Rosetta: A computer program for estimating soil hydraulic parameters with hierarchical pedotransfer functions. *J. Hydrol.* **2001**, *251*, 163–176. [[CrossRef](#)]
31. Wei, F.S.; Qi, W.Q.; Sun, Z.G.; Huang, Y.R.; Shen, Y.W. *Water and Wastewater Monitoring and Analysis Method*; China Environmental Science Press: Beijing, China, 2002; ISBN 978-7-8016-3400-9.
32. Zhang, W.Z. *Groundwater and Soil Water Dynamics*; China Hydraulic and Power Press: Beijing, China, 1996; ISBN 780-1-2413-04.

33. Tufenkji, N.; Ryan, J.N.; Elimelech, M. The promise of bank filtration. *Environ. Sci. Technol.* **2002**, *36*, 423–428. [[CrossRef](#)]
34. Metcalf & Eddy, Inc. *Wastewater Engineering: Treatment and Reuse*, 4th ed.; McGraw-Hill Inc.: New York, NY, USA, 2003; ISBN 978-0-0734-0118-8.
35. Brady, N.C.; Weil, R.R. *The Nature and Properties of Soils*, 13th ed.; Prentice Hall: Upper Saddle River, NJ, USA, 2002; ISBN 13-016763-0.
36. Aelion, C.M.; Shaw, J.N.; Wahl, M. Impact of suburbanization on ground water quality and denitrification in coastal aquifer sediments. *J. Exp. Mar. Biol. Ecol.* **1997**, *213*, 31–51. [[CrossRef](#)]
37. Essandoh, H.M.K.; Tizaoui, C.; Mohamed, M.H.A. Removal of dissolved organic carbon and nitrogen during simulated soil aquifer treatment. *Water Res.* **2013**, *47*, 3559–3572. [[CrossRef](#)] [[PubMed](#)]
38. Essandoh, H.M.K.; Tizaoui, C.; Mohamed, M.H.A.; Amy, G.; Brdjanovic, D. Soil aquifer treatment of artificial wastewater under saturated conditions. *Water Res.* **2011**, *45*, 4211–4226. [[CrossRef](#)] [[PubMed](#)]
39. DiToro, D. *Sediment Flux Modeling*; Wiley-Interscience: New York, NY, USA, 2001; ISBN 978-0-47-113535-7.
40. Machesky, M.L.; Holm, T.R.; Shackelford, D.B. *Concentrations and Potential Toxicity of Metals and Ammonia in Peoria Lake Sediments and Pore Waters*; Illinois State Water Survey Champaign: Champaign, IL, USA, 2004.
41. Wetzel, R.G. *Limnology*, 2nd ed.; Saunders College: New York, NY, USA, 1983; ISBN 978-0-19-921395-4.
42. Crites, R.; Reed, S.; Bastian, R. *Land Treatment Systems for Municipal and Industrial Wastes*; McGraw Hill Professional: New York, NY, USA, 2000; ISBN 978-0-07-061040-8.
43. Quanrud, D.M.; Hafer, J.; Karpiscak, M.M.; Zhang, J.M.; Lansley, K.E.; Arnold, R.G. Fate of organics during soil-aquifer treatment: Sustainability of removals in the field. *Water Res.* **2003**, *37*, 3401–3411. [[CrossRef](#)]
44. Reemtsma, T.; Gnirß, R.; Jekel, M. Infiltration of combined sewer overflow and tertiary municipal wastewater: An integrated laboratory and field study on nutrients and dissolved organics. *Water Res.* **2000**, *34*, 1179–1186. [[CrossRef](#)]
45. Zhang, Z.Y.; Lei, Z.F.; Zhang, Z.Y.; Sugiura, N.; Xu, X.T.; Yin, D.D. Organics removal of combined wastewater through shallow soil infiltration treatment: A field and laboratory study. *J. Hazard. Mater.* **2007**, *149*, 657–665. [[CrossRef](#)] [[PubMed](#)]
46. Lenk, S.; Remmler, F.; Skark, C.; Zullei-Seibert, N. Removal capacity of riverbank filtration and conclusions for the operation of water abstraction plants. In Proceedings of the 5th International Symposium on Management of Aquifer Recharge, Berlin, Germany, 10–16 June 2005.
47. Sharma, L.; Greskowiak, J.; Ray, C.; Eckert, P.; Prommer, H. Elucidating temperature effects on seasonal variations of biogeochemical turnover rates during riverbank filtration. *J. Hydrol.* **2012**, *428*, 104–115. [[CrossRef](#)]
48. Saunders, D.L.; Kalff, J. Denitrification rates in the sediments of Lake Memphremagog, Canada-USA. *Water Res.* **2001**, *35*, 1897–1904. [[CrossRef](#)]
49. Berg, M.; Trang, P.T.K.; Stengel, C.; Buschmann, J.; Viet, P.H.; Dan, N.V.; Giger, W.; Stüben, D. Hydrological and sedimentary controls leading to arsenic contamination of groundwater in the Hanoi area, Vietnam: The impact of iron-arsenic ratios, peat, river bank deposits, and excessive groundwater abstraction. *Chem. Geol.* **2008**, *249*, 91–112. [[CrossRef](#)]
50. Jiao, J.J.; Wang, Y.; Cherry, J.A.; Wang, X.S.; Zhi, B.F.; Du, H.Y.; Wen, D.G. Abnormally High Ammonium of Natural Origin in a Coastal Aquifer-Aquitard System in the Pearl River Delta, China. *Environ. Sci. Technol.* **2010**, *44*, 7470–7475. [[CrossRef](#)] [[PubMed](#)]
51. Wang, Y.; Jiao, J.J.; Cherry, J.A.; Lee, C.M. Contribution of the aquitard to the regional groundwater hydrochemistry of the underlying confined aquifer in the Pearl River Delta, China. *Sci. Total Environ.* **2013**, *461*, 663–671. [[CrossRef](#)] [[PubMed](#)]
52. Li, L.; Lollar, B.S.; Li, H.; Wortmann, U.G.; Couloume, G.L. Ammonium stability and nitrogen isotope fractionations for $\text{-NH}_3(\text{aq})\text{-NH}_3(\text{gas})$ systems at 20–70 °C and pH of 2–13: Applications to habitability and nitrogen cycling in low-temperature hydrothermal systems. *Geochim. Cosmochim. Acta* **2012**, *84*, 280–296. [[CrossRef](#)]
53. Norrman, J.; Sparrenbom, C.J.; Berg, M.; Nhan, D.D.; Jacks, G.; Ringdahl, P.H.; Nhan, P.Q.; Rosqvist, H. Tracing sources of ammonium in reducing groundwater in a well field in Hanoi (Vietnam) by means of stable nitrogen isotope ($\delta^{15}\text{N}$) values. *Appl. Geochem.* **2015**, *61*, 248–258. [[CrossRef](#)]
54. Possemiers, M.; Huysmans, M.; Batelaan, O. Influence of Aquifer Thermal Energy Storage on groundwater quality: A review illustrated by seven case studies from Belgium. *J. Hydrol.* **2014**, *2*, 20–34. [[CrossRef](#)]

55. Krause, S.; Tecklenburg, C.; Munz, M.; Naden, E. Streambed nitrogen cycling beyond the hyporheic zone: Flow controls on horizontal patterns and depth distribution of nitrate and dissolved oxygen in the upwelling groundwater of a lowland river. *J. Geophys. Res.* **2013**, *118*, 54–67. [[CrossRef](#)]
56. Barnes, R.T.; Smith, R.L.; Aiken, G.R. Linkages between denitrification and dissolved organic matter quality, Boulder Creek watershed, Colorado. *J. Geophys. Res.* **2012**, *117*, 1–14. [[CrossRef](#)]
57. Bekele, E.; Toze, S.; Patterson, B.; Higginson, S. Managed aquifer recharge of treated wastewater: Water quality changes resulting from infiltration through the vadose zone. *Water Res.* **2011**, *45*, 5764–5772. [[CrossRef](#)] [[PubMed](#)]
58. Regnery, J.; Barringer, J.; Wing, A.D.; Hoppe-Jones, C.; Teerlink, J.; Drewes, J.E. Start-up performance of a full-scale riverbank filtration site regarding removal of DOC, nutrients, and trace organic chemicals. *Chemosphere* **2015**, *127*, 136–142. [[CrossRef](#)] [[PubMed](#)]
59. Wang, C.; Wang, P.F.; Hu, X. Removal of COD_{Cr} and nitrogen in severely polluted river water by bank filtration. *Environ. Technol.* **2007**, *28*, 649–657. [[CrossRef](#)] [[PubMed](#)]



© 2018 by the authors. Licensee MDPI, Basel, Switzerland. This article is an open access article distributed under the terms and conditions of the Creative Commons Attribution (CC BY) license (<http://creativecommons.org/licenses/by/4.0/>).